How Much Electron Donation Is There In Transition Metal Complexes? A Computational Study

Augustine Obeng[a], Jochen Autschbach[a,*]

[a]Department of Chemistry
University at Buffalo
State University of New York
Buffalo, NY 14260-3000, USA
email: jochena@buffalo.edu

June 2, 2025

Abstract

The 'dative' covalent interactions between metals and ligands in coordination compounds, i.e., metal-to-ligand and ligand-to-metal donation, are manifestations of electron delocalization and subject to errors in approximate calculations. This work addresses the extent of dative bonding/donation in a series of closed-shell transition metal complexes. Several Kohn-Sham density functionals, representing different 'rungs' of approximations, along with post-Hartree-Fock methods are assessed in comparison to CCSD(T). Two widely used non-hybrid and global hybrid density functionals (B3LYP, PBE0) tend to produce notably too strong donation. Global hybrids with elevated fractions of exact exchange (40 to 50%) and the range-separated exchange functional CAM-B3LYP tend to perform better for the description of donation. The performance of a double-hybrid functional is found to be quite satisfactory, correcting errors seen in MP2 calculations. A fast approximate coupled-cluster model (DLPNO-CCSD) also gives a reasonable description of the donation, with a tendency to underestimate its extent.

1 Introduction

It has long been recognized that the interactions between metal centers and the ligands in coordination compounds are not just electrostatic in nature but also covalent.[1] Covalent interactions between the metal and the ligands are therefore of utmost importance to rationalize and improve upon the desired physico-chemical properties of transition metal (TM) complexes.[2,3] Despite many decades of intense research, these covalent interactions are still not fully understood. In turn, a lack of understanding hampers the advancement of the many practical applications of TM complexes.

It is safe to assume that some degree of ligand to metal (L-M) electron donation is always present in TM complexes. The donation is usually referred to as dative bonding, although the term 'donation bonding' would also be an apt description. Namely, chemical bonds of varying degree of covalency can be formed by a ligand sharing some of its electron density with the metal center. When the metal center has formally non-bonding occupied valence d-orbitals, metal to ligand donation (M-L, termed back-donation or backbonding) may also take place with π-acceptor ligands such as carbonyl. In a linear combination of atomic orbitals (LCAO) molecular orbital (MO) theoretical framework of a TM complex, both types of electron donation are readily visible as an in-phase mixing of the relevant ligand and metal AOs. Examples can be found in contemporary inorganic chemistry textbooks; see also a recent 'primer' on molecular orbital theory.[4]

Variations in the L-M and M-L donation may be of high importance for tuning a system for optimal performance, e.g., for luminescence or in a catalytic process. In principle, the donation in metal complexes ought to be observable in the case that highly accurate electron densities can be extracted from diffraction experiments. However, electron densities generated from experimental data may not be sufficiently accurate to allow the assignment of subtle variations in the donation, and furthermore the associated deformation densities depend on the definition of the promolecule. The electron density alone may also not reveal enough information about the balance of L-M donation vs. M-L back-donation. For M-L back-donation with carbonyl ligands, for example, the lowering of the C–O vibrational frequency relative to the free ligand has long been recognized as a sensitive probe, and the reason for the frequency lowering is readily rationalized by MO-theoretical concepts. For L-M donation, spectroscopic probes such as NMR chemical shifts or nuclear quadrupole interactions can be used, but their interpretation in terms of bonding/donation tends to require accurate supporting calculations. Taken together, the aforementioned points mean that quantum mechanics (QM) based calculations for metal complexes[5] play an exceptionally important role in characterizing L-M and M-L donation. Given the wide range of applications of TM complexes, an important question is therefore this: How much donation is actually present in a given system, and do quantum chemical calculations at different levels of approximation represent it accurately?

TM systems that are of practical interest tend to be large by the standards of numerical quantum chemistry.[5] It is therefore extremely important that computational methods are accurate, but also feasible in terms of the computational cost associated with the calculations. Kohn-Sham (KS) density functional theory (DFT), abbreviated here as Kohn-Sham theory (KST), is presently the only electronic structure method that can be applied to TM systems of broad interest, in a variety of application fields, without compromising unduly in terms of

the accuracy of the results or computational cost. The success of KST is rooted in its ability to treat the dynamic correlation of the electrons (albeit in an approximate manner; the exact functional is not known and may never be), while commonly applied hybrid functional KST approximations scale no worse with the system size than a calculation with Hartree-Fock (HF) theory. The latter does not treat the dynamic correlation.

Shortcomings of KST with approximate functionals have by now been well documented and recognized. Among them, the delocalization error (DE) features prominently.[6,7] With many common hybrids and especially non-hybrid functional approximations, the electronic structure is too delocalized. The DE is primarily a consequence of introducing an unphysical self-repulsion of the electrons when the exchange arising from the use of the Kohn-Sham Slater determinant is not treated exactly. As a consequence, the density may be noticeably deficient in calculations with approximate functionals that perform well for the energy or molecular structures.[8,9] The DE tends to be most pronounced with non-hybrid functionals. HF calculations, which treat the single-determinant exchange exactly but ignore the dynamic correlation, typically produce an opposite error—the electronic structure is too localized. The electrons are allowed to get too close to each other, on average, when their mutual repulsion is not treated explicitly. In the context of the present study, a localization error may be considered as a negative DE. As has been argued previously,[10] multi-configurational wavefunction methods such as complete active space self-consistent field (CASSCF) and its variants, which are widely applied in TM chemistry, likely inherit the HF localization error because the active orbital spaces are typically not large enough to treat the dynamic correlation to a meaningful extent.

The donation in metal complexes, along with the associated covalent bonding, is a form of electron delocalization, and therefore, it is impacted directly by the DE. As shown in Reference 7 and literature cited therein, energy-based measures for the DE correlate directly with the delocalization of the system's orbitals or a subset thereof. Based on the preceding discussion, presumably the correct degree of donation, be it of the L-M or M-L type, is more extensive than what is predicted by HF theory but typically exaggerated in KST calculations.[11] The situation thus compels the previously stated question, that is, how much of the donation obtained via a quantum chemical calculation is physical?

The present study was undertaken to provide an answer to this important question for TM complexes. Previous work by our group along these lines[12] considered the extent of donation into the 4f shell of certain lanthanide ions in a small number of complexes. The study was limited in scope and did not explicitly consider the effects of density relaxation in the correlated reference calculations. Herein, we provide an extensive investigation of the extent of donation in metal complexes, by studying a series of representative 6-coordinate complexes

of Fe, Co, Ru, and Rh with chloride, ammonium, carbonyl, and cyano ligands. A representative subset of the structures is shown later, in Figure 1. High-symmetry structures with only one type of ligand per complex are considered in this work to simplify the quantification of donation and back-donation. KST calculations are compared with fully relaxed densities from coupled-cluster singles and doubles (CCSD) as well as CCSD with pertubative triples [CCSD(T)]. The latter if often, if somewhat inappropriately (considering that in economics the gold standard is deprecated), referred to as the 'gold standard' of quantum chemistry. In other words, in combination with suitable basis sets, CCSD(T) gives accurate molecular energies and properties that are deemed to be quite close to the exact solution of the electronic Schrödinger equation. In addition to comparing CCSD(T) with various KST approximations, we also provide results from calculations with a fast coupled-cluster variant known as domain-based local pair natural orbital CCSD (DLPNO-CCSD), 2nd-order Møller-Plesset perturbation theory correlation (MP2), and a double-hybrid functional mixing KST-based and MP2-based correlation. It is shown that non-hybrid KST and functionals with 20 to 25% exact exchange (eX) produce too much (back-) donation. Global hybrids with up to 50% eX and the range-separated exchange hybrid CAM-B3LYP perform better in this regard. The double-hybrid also produces relative accurate extents of (back) donation. DLPNO-CCSD is shown to give a reasonable approximation of dative bonding, with a tendency to underestimate its extent.

2 Computational Details

The study mainly used the following software packages: Gaussian 2016 (G16),[13] NBO version 6,[14,15] ORCA 5.0,[16] and Molpro version 2023.2.[17–19] Spin-singlet closed-shell ground state structures of the complexes were optimized with G16, using the hybrid B3LYP functional[20] and the all-electron polarized valence-triple zeta basis def2-TZVP.[21–23] The D3(BJ) dispersion correction with Becke-Johnson damping[24,25] was used as well for the optimizations. Vibrational analyses were performed to verify that the structures are local minima; no imaginary frequencies were present. A 'veryTight' SCF convergence was set. We chose the B3LYP-D3(BJ)/def2-TZVP level because of its known excellent performance and a good compromise between accuracy and computational cost for geometry optimizations of small and large molecules.[26–30]

Using the same basis set, combined with def2/C auxiliary basis set[31–34] for domain-based local pair natural orbital coupled-cluster calculations and the def2/J[35] auxiliary basis for all methods, calculations and analyses were performed using the ORCA and NBO6 programs to investigate the impact of the DE on the extent of donation. Test calculations for Fe, Co, Ru,

Rh with ligands CO, Cl^-, NH_3, and CN^-, respectively, showed that the use of the auxiliary basis set did not have a significant impact on the values reported herein for the (back-) donation, with differences found in the third or fourth decimal place. Among the approximate functionals used for the study were the non-hybrid approximation BLYP,[36,37] the hybrid functionals B3LYP [parametrization as in the Gaussian code, 20% exact exchange (eX)], PBE0[38] (25% eX), PBE0 variants with 40% or 50% eX (PBE0-X with X = 40, 50), BHLYP (50% eX) and HF (100% eX, no correlation functional). The Coulomb-attenuated method (CAM) variant of B3LYP (CAM-B3LYP)[39] was considered as a representative of hybrid functionals with range-separated exchange. The fraction of eX in CAM-B3LYP depends on the inter-electronic distance and ranges from 19% at short range to 65% in the long-range limit. The conductor-like polarizable continuum model, CPCM,[40,41] was used in a subset of the calculations to investigate the influence from the environment such as solid-state embedding or a solvent.

KST calculations were compared to NBO analyses based on ORCA calculations of the relaxed densities[42] obtained from a 'parameter-free' PBE-based double-hybrid, PBE0-DH, with 12.5% MP2 admixture[43] as well as standard MP2 theory,[44–46] using the same def2-TZVP basis as employed in the KST calculations. We also investigated the linearized densities from domain-based local pair natural orbital coupled-cluster with singles and doubles (DLPNO-CCSD)[47] calculations, as well as densities from orbital-optimized coupled-cluster with doubles (OO-CCD),[48] as generated by ORCA. The latter calculations are not explicitly discussed herein, except for noting here that test calculations using the smallest complexes in the set were performed to ascertain that the OO-CCD calculations with ORCA produced orbital population data that were virtually identical to those from fully relaxed CCSD as implemented in G16. Likewise, the data collection in the Supporting Information (SI), in particular Table S3, shows that the OO-CCD implementation in ORCA gives very similar results to the relaxed CCSD calculations with Molpro. Finally, all-orbital correlated fully relaxed CCSD[49] and CCSD(T)[50] densities were calculated using Molpro, also using the def2-TZVP basis. Table 1 summarizes the electronic structure methods used in this study. T1 diagnostics for the set of complexes ranged between 0.0107 and 0.0324; these are considerably lower than the recommended thresholds of 0.05 for 3d TM systems[51] and 0.045 for 4d TM systems.[52] Therefore, the ground states of the complexes studied herein do not give cause for concerns due to multi-configurational character.

The extent of donation and back-donation was explored numerically based on natural population analysis (NPA) and the extent of delocalization of natural localized molecular orbitals (NLMOs) as obtained from NBO calculations.[14] Further details are provided in the Results and Discussion section. To keep the number of calculations manageable, we opted to focus in this study on two group-8 metals, Fe and Ru, and two group-9 metals, Co and

Table 1: Description of the electronic structure methods used in this study.

Method	Description
BLYP	KST with a non-hybrid generalized gradient approximation (GGA) density functional combining the Becke '88 exchange functional and the Lee-Yang-Parr (LYP) correlation functional.[36,37]
B3LYP	KST with a global hybrid GGA functional[20] with 20% exact exchange, based on Becke and LYP GGA exchange and correlation functionals. The parameterization of the functional is detailed in Ref. 53.
PBE0	KST using a global hybrid GGA functional with 25% exact exchange,[38] based on Perdew-Burke-Ernzerhof GGA exchange-correlation functional.[54,55]
PBE0-50	KST with a PBE0 variant mixing 50% DFT exchange with with 50% exact exchange.
BHLYP	Global hybrid GGA functional[20] based on Becke and LYP exchange and correlation functionals, with 50% exact exchange,[56] 50% Becke '88 exchange, 50% LDA exchange and 100% LYP correlaion
CAM-B3LYP	KST using a hybrid-GGA functional with range-separated exchange ('Coulomb-attenuated method') based on B3LYP.[39] The fraction of exact exchange is 19% in the short-range limit (interelectronic distance) and 65% in the long-range limit.
HF	Hartree-Fock theory. The wavefunction is a single Slater determinant. Exchange is treated exactly; dynamic correlation is absent.
MP2	Starting with a HF calculation, dynamic correlation is treated by second-order perturbation theory.[44–46]
PBE0-DH	Generalized KST with a double hybrid[57] functional. PBE0 with 12.5% admixture of MP2 correlation.[43]
CCSD	Correlated post-HF wavefunction method. Coupled-cluster with singles and doubles substitution.[49]
CCSD(T)	CCSD with perturbative correction for connected triples.[50]
DLPNO-CCSD	Domain-based local pair natural orbital CCSD.[47] Densities are linearized.
OO-CCD	Coupled cluster doubles with orbital optimization.[48]

Rh, combined with the strong-field ligands CO and CN^- vs. the weak-field ligands Cl^- and NH_3. Six-coordinate complexes $[ML_6]^n$, where M is the metal and L is the ligand, octahedral or nearly octahedral (NH_3 ligands) in symmetry, were optimized at a reliable level of theory and confirmed as local minima on the potential energy surface via calculations of harmonic vibrational frequencies. The optimized geometries are provided in section S1 of the SI and were used for all subsequent calculations. Hexachloroferrate(II) was excluded from the test set because optimizations did not locate a stable gas-phase minimum structure, although the complex is known to exist in condensed phase.[58] With the geometries fixed at the B3LYP-D3(BJ)/def2-TZVP level, variations in the extent of L-M donation, and M-L back-donation where applicable, for a given system therefore result from the approximations in the electronic structure models. The electronic structures of the complexes correspond to a closed-shell low-spin d^6 configurations. The L-M σ donation therefore affects the metal d orbitals of

e_g symmetry (the actual symmetry, or its e_g parentage), whereas M-L π back-donation takes place from the three occupied non-bonding t_{2g} metal d orbitals.

3 Results and Discussion

Reference Data: The relaxed CCSD(T) calculations represent the highest correlated ab-initio level that can presently be deemed practical for the purpose of this benchmark, and they will be used as references for the extent of L-M and M-L donation. These calculations are not at the complete-basis set (CBS) limit. However, we consider CCSD(T)/def2-TZVP as a suitable choice and a good compromise, with the results likely not being far from the exact limit, to gauge the performance of other types of calculations with the same basis sets and to address the extent of donation and back-donation in metal complexes. It is very important to use the same basis set consistently when evaluating the donation trends among sets of different calculations; otherwise, the comparisons will be obscured by the mild but non-negligible basis set dependence of the NPA (vide infra).

We evaluated the T1 diagnostic[59] in the coupled-cluster calculations to assess the reliability of our reference wave functions. The T1 diagnostic is a scaled norm of the vector of amplitudes in the operator for one-particle excitations in the coupled-cluster *ansatz* and provides a quantitative measure of the multi-configurational character of the wavefunction and therefore the suitability of a single-reference correlation treatment, for example, by CC calculations. The calculated T1 diagnostics for the complexes in this study were well below the recommended thresholds of 0.05 for 3d TM systems and 0.045 for 4d TM systems (criteria determined by Jiang et al.[51] and Wang et al.[52] respectively). This is a strong indication that the reference wavefunction is dominated by a single configuration and therefore single-reference correlation methods are appropriate.

The CCSD(T) reference calculations used for this study are presently not compatible with the use of an embedding model such as CPCM. Therefore, the question posed in the article's title is addressed via consistent sets of calculations for isolated molecules ('gas phase'). However, it is important to assess how the extent of donation varies when the environment is considered—in particular for anionic systems. A polar or polarizable medium plays an important role in the stabilization of ionic complexes. Using gas-phase optimized structures, we evaluated the influence of the environment by using the CPCM embedding model with an infinite dielectric constant (DC) as well a DC of 80 corresponding to water at room temperature, in combination with the BHLYP functional. [As shown later, BHLYP predicts L-M and M-L donation reasonably well.] Results for a subset of the complexes are collected in Table S5 in the SI. For anionic complexes with CN^- ligands, the difference in the donation is

negligible [on the order of 10^{-3}]. The difference is somewhat larger, between 0.04 and 0.1, for the Cl^- coordinated complexes but still not large. We also examined how the extent of donation changes in the presence of an embedding model when using structures optimized in the presence of CPCM embedding (DC $\rightarrow \infty$). The data are collected in Table S6 and display similarly weak trends as noted for the CPCM effects noted for the gas phase optimized structures. To reiterate, the main focus of the present study is to learn how much donation is present in metal complexes according to a highly accurate level of theory, and how well this is approximated at commonly used but more approximate levels. Based on our test calculations, the trends obtained for isolated systems are representative of the trends that would be seen in a medium representing a stabilizing solvent or crystal embedding. Consequently, in what follows we discuss the gas phase data, such that a fair comparison with CCSD(T) can be made.

Numerical Evaluation of the Extent of Donation: As alluded to in the Introduction, there is no unique QM partitioning of the electron density, in the sense that the partitioning of electrons to specific atoms or atomic shells in a molecule has no associated well-defined self-adjoint QM operator. Therefore, the assignment of L-M and M-L donation in a metal complex has to rely on chemically intuitive concepts that are embedded in a QM framework for calculations. Older[60] and more recent[61] work has shown that most of the criteria for atomic charges, for instance, probe mainly the same underlying physics. The natural population analysis (NPA) produced by the NBO program was identified as one among several criteria based on the generation of atomic orbitals in molecules that give consistent results[61] without excessive sensitivity to the choice of the AO basis for the calculation. We, therefore use NBO-based criteria in the present work to compare different levels of calculations for a given complex. Note that the subset of NBO algorithms used in the present work only require the (1-particle) density matrix along with the basis set specification and overlap matrix, which is therefore equally applicable to KST and correlated wavefunction calculations. As mentioned, the AO basis should be the same in the different calculations, such as to avoid spurious trends that may arise from a sensitivity, even if it is weak, of the chosen partitioning to the basis set definition.

Specifically, the extent of L-M σ donation was obtained from the combined metal density weights of the six relevant σ-donating occupied natural localized MOs (NLMOs). In KST calculations, the latter are obtained as linear combinations of the occupied 'canonical' MOs (the usual MOs generated by self-consistent field calculations) such as to create spatially compact molecular orbitals that represent individual bonds, lone pairs, and core shells. See Reference 14 for an overview. In a similar vein, the extent of M-L π back-donation was quantified via the

loss of electron density in the three formally non-bonding t_{2g} metal d orbitals as represented by the corresponding NLMOs. The correlated post-HF wavefunction methods produced similar sets of bonding and lone-pair NLMOs as the KST calculations, albeit with non-integer occupations slightly below 2. Consequently, the occupation deviations from 2 were factored into the donation data. Small residual errors in the extent of (back-) donation that arise from not considering additional orbitals with small occupations (from the correlation treatment) that may have bonding or antibonding character are estimated to amount to less than 1% of the values reported herein and therefore negligible in the context. The orbital-based analysis of donation has the advantage that the L-M σ donation can reliably be separated from the M-L π back-donation. A minor disadvantage of the chosen analysis is that the orthogonality of the NLMOs requires them to have orthogonalization 'tails' on other atoms. In the context of the present study, this means a ligand lone pair NLMO, even if it is not actually donating, will have a small percentage of its density on the metal because of the orthogonality. However, we assume that a 'pre-donation' orthogonality creates roughly the same offset for all of the electronic structure methods that were used, such that the *variations* in the donation, as extracted from the NLMO analysis, are reliable indicators for the extent of delocalization predicted by the calculations.

L-M σ Donation: It is beneficial to delineate how the NBO algorithms assign the L-M dative bonding in the types of complexes studied herein. Typically, a given ligand L and its counterpart in *trans* position create a 3-center 4-electron (3c4e) bond with the metal M according to the following—more or less pronounced—resonance:

$$\text{L:}\quad \text{M—L} \qquad \longleftrightarrow \qquad \text{L—M}\quad \text{:L}$$

In an octahedral complex, there are accordingly three pairs of 3c4e bonds of this type. The default NBO algorithms assign for each of them an orbital description that corresponds to one of the resonance structures. In this case, the strongly localized 'parent NBOs' of the NLMO pair describing the 3c4e bond come as a lone pair (LP) and a bond (BD). The corresponding NLMOs are both bonding, however, although not completely equivalent. It is important to note that this does not indicate symmetry-breaking; it is simply that the other resonance structure is not also created by default. The bond orders, for example, that are calculated by the NBO program are the same for bonds that are symmetry-equivalent, which we verified for the present systems. In the context of this study, the metal density weights for the LP and BD NLMOs were added for the three pairs. Figure 1 shows visualizations of the six σ-donating NLMOs of four representative complexes. Table S1 in the SI lists for the B3LYP

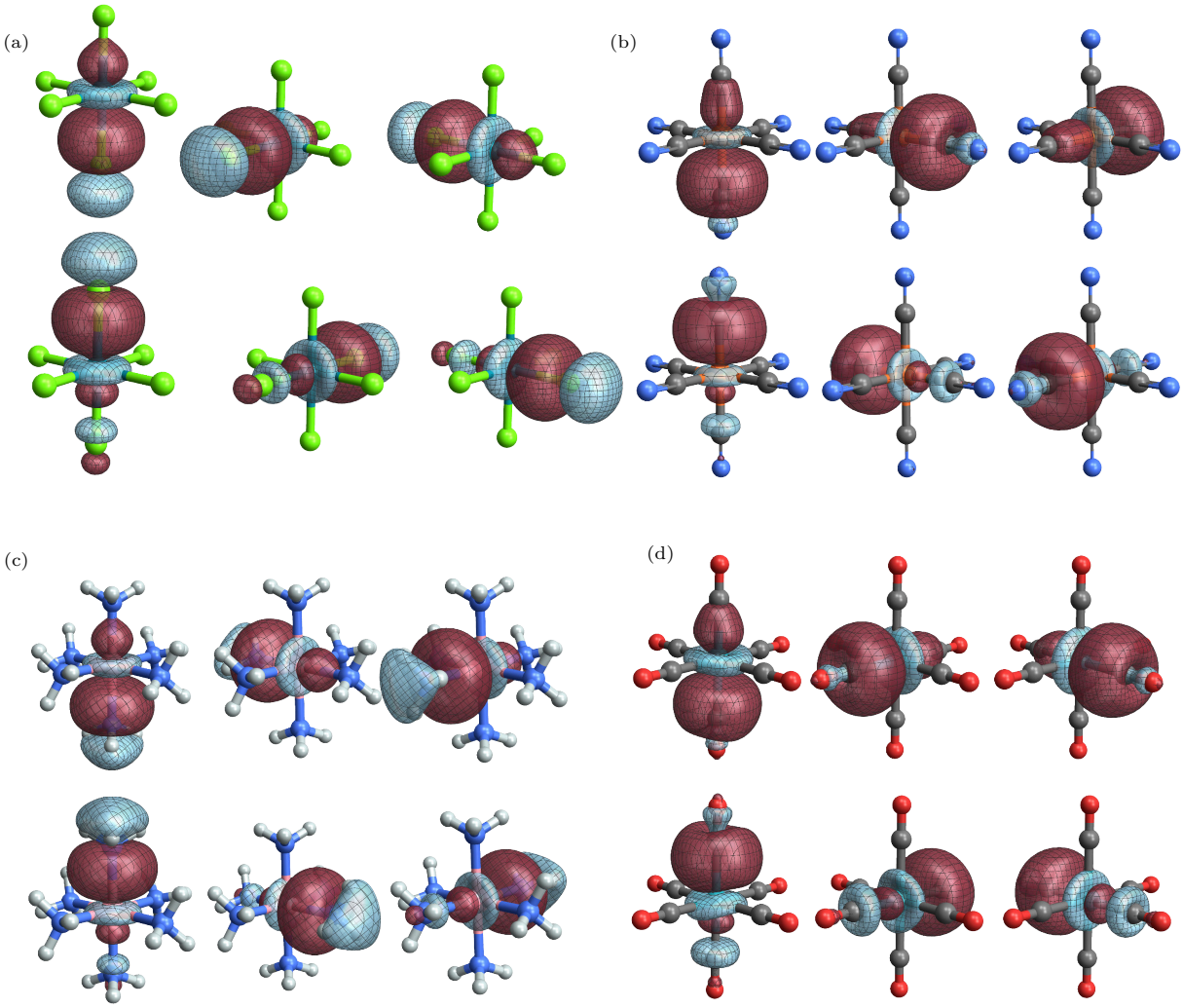

Figure 1: Isosurface representation of σ-donating NLMOs of selected metal complexes at B3LYP/def2-TZVP level. Iso value ± 0.03. The first three NLMOs in each panel have bond (BD) assignments of their parent NBOs; below them are the three corresponding lone-pair (LP) NLMOs. (a) $[Rh(Cl)_6]^{3-}$, (b) $[Fe(CN)_6]^{4-}$, (c) $[Co(NH_3)_6]^{3+}$, and (d) $[Ru(CO)_6]^{2+}$.

calculations the aggregate donation for the LP vs. BD σ NLMOs. The sum of the two entries shows up in Table S2 as the total amount of σ donation for the B3LYP calculation of a given complex. Data for the other complexes and other functionals were assembled in the same manner. Results from KST calculations for all of the complexes are displayed in the form of bar graphs in Figure 2.

The results displayed in Figure 2 are clear and compelling. The broad trend is that approximate functionals tend to produce a lower extent of donation with higher fractions of eX. At one extreme end is BLYP (no eX, approximate DFT exchange and correlation functionals), which always gives the largest extent of donation. At the other extreme is HF theory (eX only,

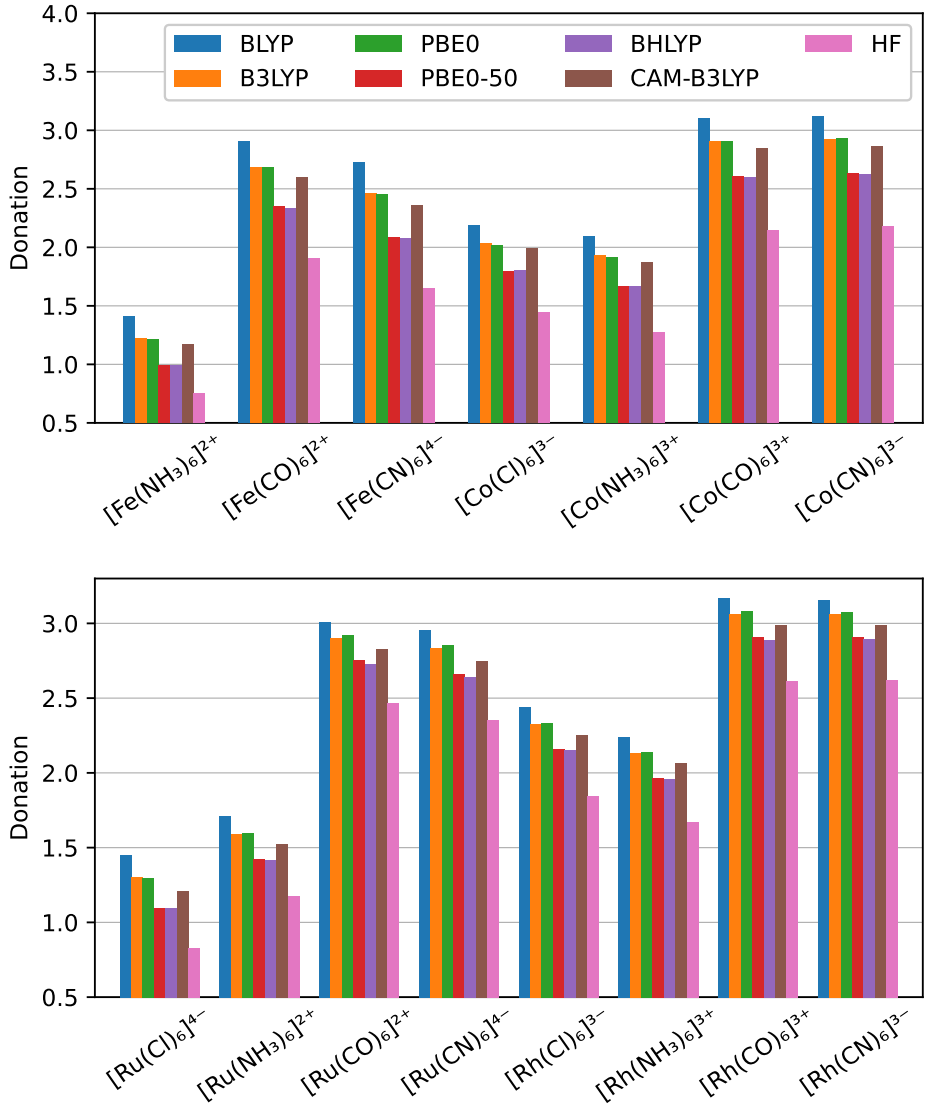

Figure 2: Extent of L-M donation (integrated donated electron density, from NLMO analysis) in KST calculations with different functionals

no dynamic correlation), which gives the least donation. Those are clear manifestations of the Kohn-Sham DE for BLYP vs. the localization error of HF theory. The functionals B3LYP (20% eX) and PBE0 (25% eX) produce less donation than BLYP but stronger donation than the 'half-half' (50% eX) functionals PBE0-50 and BHLYP. CAM-B3LYP, which features range-separated exchange, gives an extent of donation that is between the B3LYP/PBE0 group and the 50% eX functionals and tends to be closer to the former. The specific form of the exchange-correlation functional matters, but not a lot, as exemplified by the similarity of the data for BHLYP and PBE0-50, which both have 50% eX. The comparison of B3LYP and PBE0 is also useful. It is seen that the donation is not always higher with B3LYP than PBE0, even though

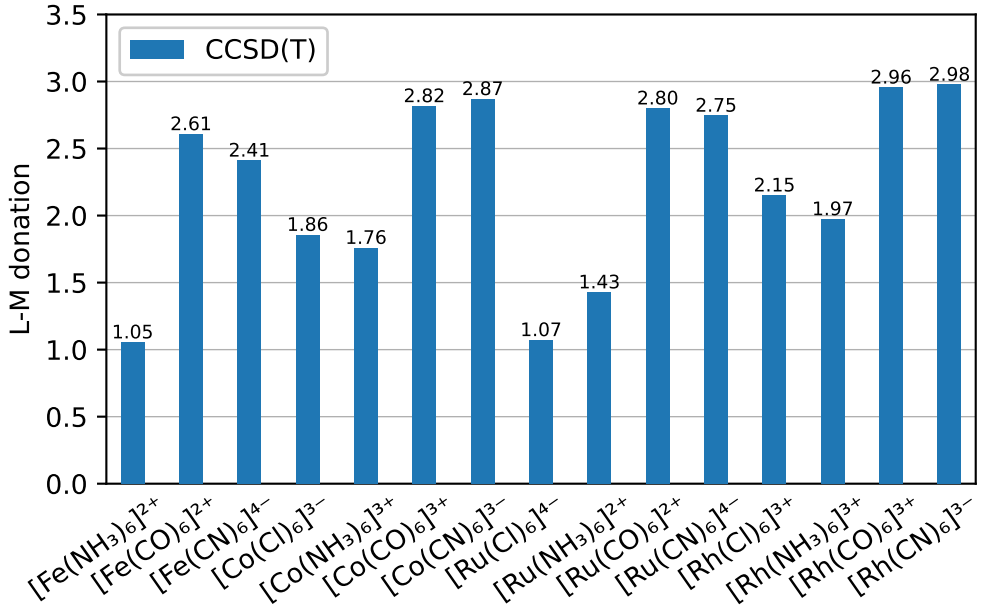

Figure 3: Extent of L-M donation (integrated donated electron density, from NLMO analysis) in the CCSD(T) calculations.

this approximate functional has a bit less eX than PBE0. However, the differences in the L-M donation between these functionals, and between BHLYP and PBE0-50, are likely close to the margins of error of the chosen analysis method (refer to the caveats discussed earlier regarding the NLMO orthogonality, for example). Overall, it is clear that the extent of L-M donation in KST calculations varies considerably with the approximations made in the functional and primarily with the fraction of eX.

Other trends in Figure 2 relate to the chemistry of the systems. Ligands CN^- and CO are strong σ donors with the selected metals, whereas ammonia and chloride donate considerably less density to the metal. For a given ligand, substituting a 3d metal with a 4d metal from the same group (Fe → Ru, Co → Rh) results in stronger donation. It is therefore important to address the question: Which of the calculations displayed in Figure 2, if any, has the right amount of L-M donation?

To answer this question, we turn to Figures 3 and 4. Figure 3 displays a bar chart with the extent of L-M donation generated via the relaxed CCSD(T) calculations. Figure 4 shows how the L-M donation in the other calculations differs from CCSD(T), with the latter assumed to be close to the exact limit (full correlation, CBS). The main takeaway from Figure 3 is that the extent of donation is considerable, between 1 and 3 electrons in aggregate. The chemical trends extracted from the KST calculations are reflected in the CCSD(T) results: There is weaker donation for NH_3 and Cl^- as compared to CO and CN-, and for a given ligand there is stronger donation to a 4d metal as compared to a 3d metal from the same group.

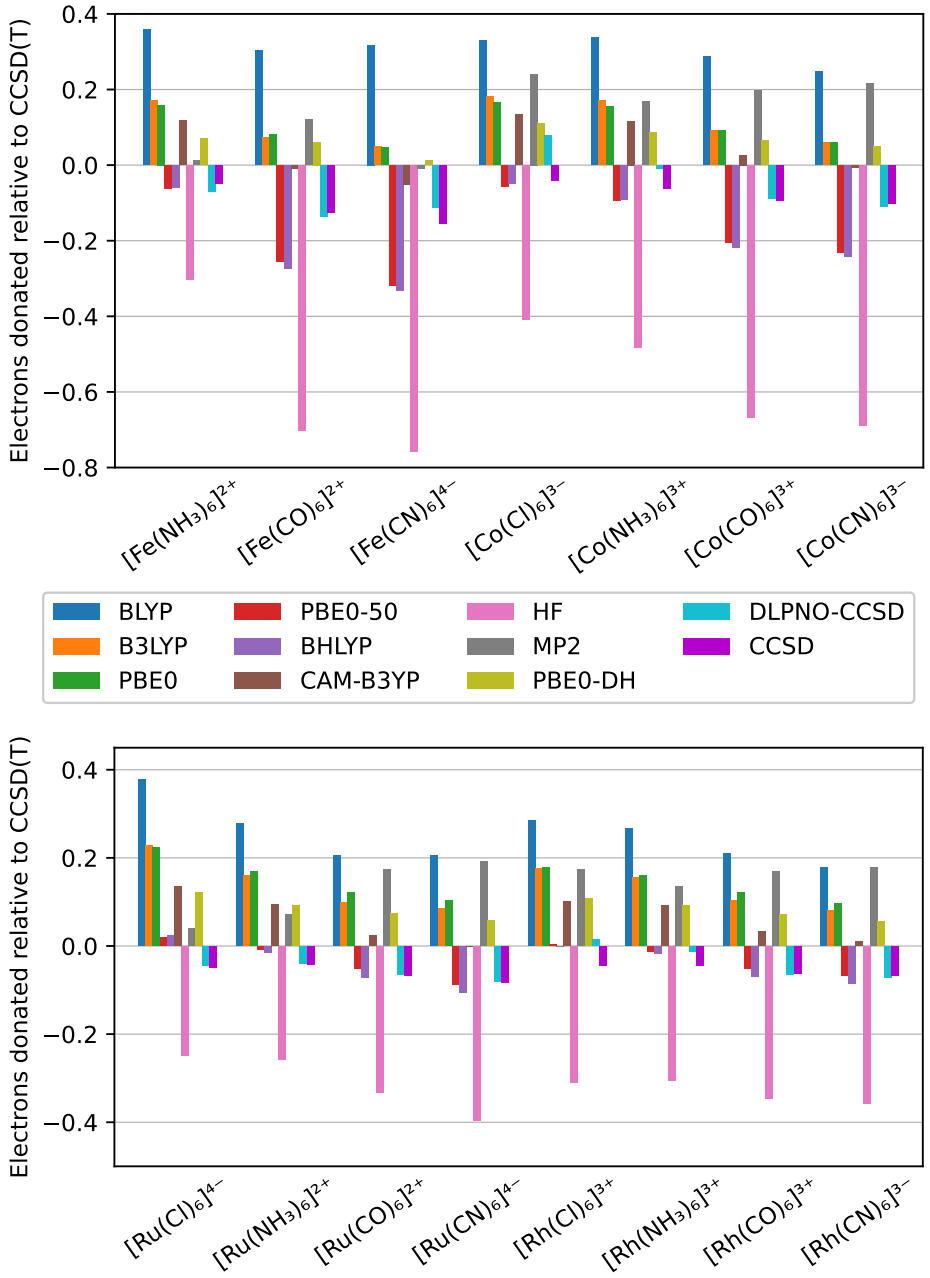

Figure 4: Extent of L-M donation obtained from different electronic structure methods relative to CCSD(T).

Figure 4 reaffirms that KST with the non-hybrid functional (BLYP) and HF theory produce large errors of opposite signs, as expected from the preceding discussion. In most cases, HF produces a larger-magnitude localization error than the magnitude of the DE generated by BLYP. MP2 is the least costly (in terms of required computational resources) post-HF correlated wavefunction method. It is therefore interesting to note that relative to CCSD(T) the MP2 calculations produce in most cases rather pronounced positive errors in the extent of

L-M donation, more often than not exceeding those from CAM-B3LYP. The error is in the opposite direction from HF theory. It is sometimes said that MP2 tends to over-correct for the lack of correlation, and it appears that this can also be the case for the L-M donation in metal complexes. Where HF theory has a large localization error, MP2 therefore gives too much delocalization akin to some of the approximate density functionals. In two of the iron complexes (with NH_3 and CN^- ligands, respectively, MP2 is spot-on with the CCSD(T) reference, which is potentially fortuitous.

As we have seen, KST with the functionals PBE0 and B3LYP gives a similar extent of L-M donation. It has also been argued that these functionals produce accurate electronic structures, for example, because they produce verifyably accurate molecular geometries.[28,62] or NMR parameters.[63,64] However, Figure 4 and additional data provided in Table S3 demonstrate that these functionals uniformly over-estimate the extent of L-M donation, albeit much less strongly than non-hybrid KST, by about 0.1 to 0.2. More often than not, the global hybrid functionals with 50% eX perform better, with a similar error as CCSD. It needs to be noted, though, that, the 50% eX global hybrids perform rather poorly for the 3d metals Fe and Co interacting with the ligands CN^- and CO. In these cases, the L-M donation error is greater than 0.2 electrons combined for the six ligands and negative. In other words, the donation strength is underestimated in these cases and B3LYP or PBE0 would be better choices.

Interestingly, the double-hybrid, combining MP2 correlation with a PBE-based hybrid functional, performs comparatively well for L-M donation when compared to the CCSD(T) benchmark, usually (although not always) better than MP2 or PBE0 individually. Based on the present data, one may therefore expect the double-hybrid to perform better than MP2, at comparable computational cost, when it comes to the description of M-L donation. The range-separated exchange functional CAM-B3LYP also performs quite well overall, often producing results comparable to the PBE0-based double-hybrid. The deviations with respect to CCSD(T), for the cases when they are not negligibly small, are uniformly in the positive direction, both for the double-hybrid and for CAM-B3LYP, i.e., both tend to produce a residual DE.

Finally, it is interesting to compare the densities from the DLPNO-CCSD implementation in ORCA, and the relaxed CCSD results, with the CCSD(T) reference. DLPNO-CCSD makes use of the sparsity of the density matrix to apply approximations that can considerably speed up the calculations, although shortcomings have been noted.[65–67] In the context of our study, it is important to note that the DLPNO approximation indeed significantly speeds up the calculations, but only a 'linearized' relaxed density is available in its current implementation.[68] As seen in Figure 4, the extent of L-M donation in DLPNO-CCSD is often very close to relaxed CCSD and appears to perform well overall, without producing severe outliers compared to

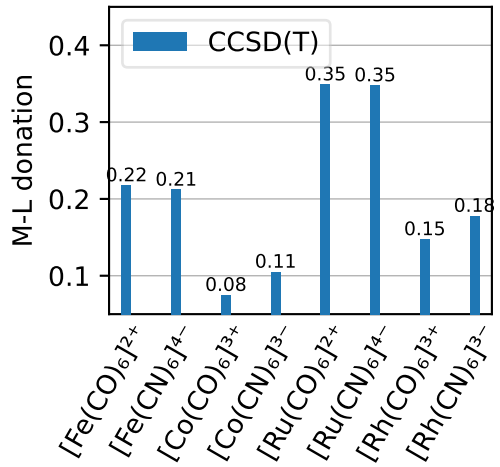

Figure 5: Extent of M-L back donation (integrated donated electron density, from NLMO analysis) in the CCSD(T) calculations.

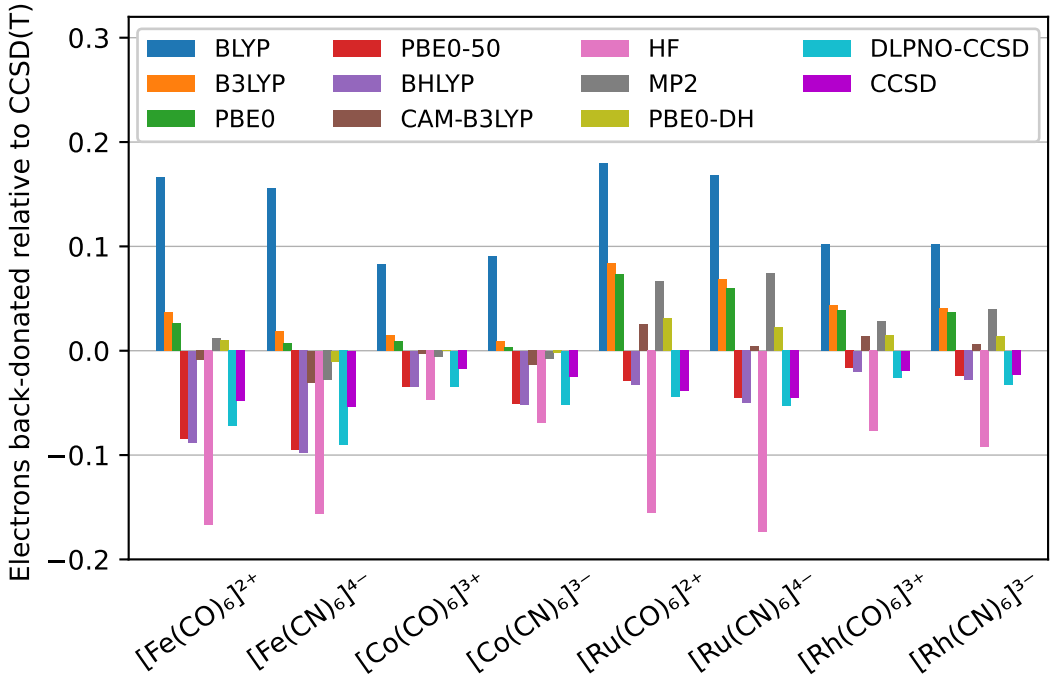

Figure 6: Metal-Ligand π-back-donation from various methods relative to CCSD(T).

CCSD. The latter uniformly gives a small localization error when compared to CCSD(T). The deviation from CCSD(T) is always less than –0.2 in magnitude and usually below –0.1. The additional correlation afforded by the (T) corrections is therefore seen to produce a bit more L-M covalency/donation.

M-L π Back-Donation: For the complexes with π-acceptor ligands, Figure 5 shows the extent of M-L back-donation in the CCSD(T) reference calculations. Figure 6 displays a chart with the differences in back-donation from all other calculations relative to CCSD(T). Similar trends as noted for the dependence of L-M σ donation on the level of theory can be observed when considering the M-L π back-donation. Namely, there is also a broad trend of too much back-donation with non-hybrid functionals, too little back-donation with HF theory, and the CCSD(T) benchmark and the remaining theoretical models are in between. The reason for these findings is that the underlying driver—delocalization—is the same for L-M donation and M-L back-donation, although, of course the nature of the donor and acceptor orbitals differs.

Also, in keeping with the broad trend of the eX fraction determining much of the extent of delocalization, the 50% eX global hybrids PBE0-50 and BHLYP give very similar results for the M-L back-donation. The smaller data set for M-L back-donation shows a more systematic trend for the B3LYP (20% eX) vs. PBE0 (25% eX) comparison in that B3LYP systematically gives slightly more back-donation in keeping with the lower fraction of eX in the functional. However, the differences are small and perhaps they do not exceed the numerical uncertainties of the analysis. CAM-B3LYP and the double-hybrid perform very well for the back-donation cases studied herein. As in the case of the L-M donation, CCSD and DLPNO-CCSD are seen to produce similar extents of M-L back donation, and CCSD has a (relatively minor) localization error relative to CCSD(T). We note in passing that the difference between the aggregate M-L σ donation into the metal e_g d orbitals and the aggregate M-L π back-donation from the metal t_{2g} d orbitals is very close to the difference between the formal charge of the metal centers and the calculated metal charges from the natural population analysis (NPA) (see Tables S7 and S8 in the SI).

Using a 40% eX global hybrid: The trends in Figure 4 suggest that a reasonable description of the L-M donation may be obtained with global hybrids that have eX fractions between 20/25% and 50%. Incidentally, it has been seen occasionally that eX fractions higher than 20 or 25 percent can be beneficial for calculating the NMR chemical shifts of ligands directly bound to f-elements.[69,70] We note this here with the caveat that in some cases the higher eX fraction compensated for another approximation in the NMR calculations,[71] and with the caveat that there appears to be no simple relationship between the accuracy of calculated NMR chemical shifts and the Kohn-Sham DE.[72] Nonetheless, Figure 7 shows that a 40% eX PBE-based global hybrid functional gives a reasonably good approximation of the donation in comparison to CCSD(T) across the set of complexes, even though the 3d-metal complexes with CO and CN^- ligands continue to give comparatively large deviations.

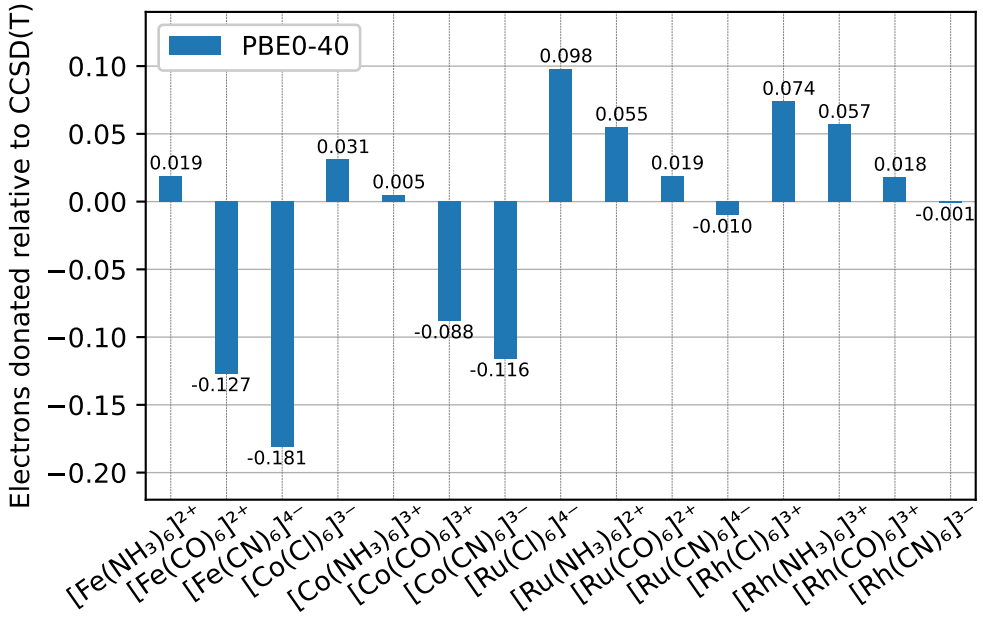

Figure 7: Calculated extent of donation with PBE0-40 relative to CCSD(T).

4 Conclusions and Outlook

In quantum chemical calculations, the extent of L-M donation and M-L back-donation in TM complexes is sensitive to the approximations made in the electronic structure model. As shown herein for a set of closed-shell group-8 and -9 TM complexes, in comparison with CCSD(T) fully relaxed densities, non-hybrid and popular hybrid density functionals predict too much donation and back donation, which can be traced back to the Kohn-Sham DE. Among the KST functional choices that are widely available in electronic structure programs, global hybrids with 50% eX or perhaps somewhat less tend to perform a little better. The range-separated exchange hybrid functional CAM-B3LYP also produced comparatively small errors for the extent of donation and back-donation, with a tendency for over-delocalization. HF theory is strongly deficient in the opposite sense, by predicting too little donation and back-donation.

Among the available post-HF wavefunction methods, MP2 tends to over-correct upon HF theory and produces donation values that appears to be no better than those obtained with KST and the B3LYP or PBE0 functionals. CCSD is overall quite close to the CCSD(T) benchmark but tends to deliver weaker dative bonding. In other words, the additional dynamic correlation afforded by the (T) corrections in the coupled-cluster calculations increases the delocalization that underlies the dative bonding. OO-CCD (see data in the SI) gives, as expected, results that are compatible with relaxed CCSD. In most cases, the linearized (approximate)

relaxed density from the DLPNO-CCSD calculations are in close agreement with CCSD. This finding is promising, because DLPNO-CCSD is applicable to considerably larger systems than CCSD, which, in turn, is less demanding than CCSD(T). Most likely, the extent of donation and back-donation obtained from DLPNO-CCSD calculations will afford a relatively minor localization error, that is, the dative bond covalency will be underestimated but not strongly so. This, of course, assumes that CCSD(T)/def2-TZVP relaxed densities are closer to the exact densities than the differences between CCSD and CCSD(T) obtained with the same basis sets.

It is improbable that a 'magic' predetermined fraction of eX in any global hybrid will produce accurate extents of metal-ligand covalency across a wide range of types of complexes. KST applications that require an accurate description of the delocalization underlying the dative bonding in metal complexes will therefore require careful benchmarking for specific targeted systems and applications. Likely, in such cases researchers will have to resort to functional parametrizations that are chosen for specific systems, for example, by varying the fraction of eX in global hybrids[73] or by non-empirical 'optimal tuning' of functionals with range-separated exchange.[7,74] In the context of generalized KST, a more universal [not molecule-(class)-specific] approach beyond the 'rung'[75] of global hybrid or range-separated exchange hybrid functional will most likely be needed to improve the description of dative bonding systematically. For example, local hybrids where the eX fraction depends on the electron positions[76,77] would seem promising in this context. Our results obtained with a PBE-based double hybrid (DH) functional, which mixes MP2 with KST correlation, appear very promising based on the present set of calculations. As mentioned in the Results and Discussion section, the DH tends to correct for the errors seen in plain MP2 calculations, and the overall aggregate error in the donation relative to CCSD(T), counting all bonding or back-bonding interactions, does not much exceed 0.1 electrons in the worst cases. To reiterate, it is imperative that relaxed densities are generated from DH, MP2, and the CC calculations. (For KST approaches, we assume that variational self-consistent calculations are employed.)

This study has focused on TM complexes with closed-shell ground states. The donation in open-shell complexes is of course also impacted by the approximations in the theoretical model, and furthermore, there are very important consequences regarding the resulting spin density in open-shell systems.[5,7] The extent of donation overall, and in particular the balance of donation in the α and β spin channels, deserve further scrutiny and might benefit from a similar investigation as was carried out here for closed-shell complexes. However, an efficient 'relaxed' CCSD(T) code for open-shell systems that can be applied to molecules of the size as studied herein is not presently available. However, we recognize this as an area of potential expansion and aim to incorporate open-shell systems in our future investigations.

Another potential avenue for study would be closed-shell square-planar d^8 systems with metals such as Pd or Pt. However, such systems possess open coordination sites which—in most laboratory settings—are coordinated by solvent molecules or counter ions, or via stacking in solids. The potential interference with the equatorial donation and back-donation requires careful investigation, which is beyond the scope of the present study and will be considered in future work.

Supporting Information

Optimized XYZ coordinates for the complexes, numerical data for the L-M and M-L donation, results from additional test calculations (PDF)

Notes

The authors declare no competing financial interests.

Acknowledgments

We acknowledge the Center for Computational Research (CCR)[78] at the University at Buffalo for providing computational resources. This work has received support from the National Science Foundation, grant CHE-2152633.

References

[1] Huheey, J. E. *Inorganic Chemistry. Principles of Structure and Reactivity;* Harper & Row: New York, NY, 3rd ed.; 1983.

[2] Dekock, R. L.; Gray, H. B., Eds.; *Chemical structure and bonding;* University science books: Sausalito, California, 1989.

[3] Figgis, B. N.; Hitchman, M. A. *Ligand Field Theory and its Applications;* Wiley-VCH: New York, 2000.

[4] Morgante, P.; Autschbach, J. *Molecular Orbitals;* American Chemical Society: Washington (DC), 2023.

[5] Autschbach, J. Quantum Chemistry of d- and f-block Elements. In *Comprehensive Computational Chemistry*, Vol. 1; Boyd, R.; Yanez, M., Eds.; Elsevier: Amsterdam, 2024 177–192.

[6] Cohen, A. J.; Mori-Sánchez, P.; Yang, W. Challenges for Density Functional Theory. *Chem. Rev.* **2012**, *112*, 289–320.

[7] Autschbach, J.; Srebro, M. Delocalization error and 'functional tuning' in Kohn-Sham calculations of molecular properties. *Acc. Chem. Res.* **2014**, *47*, 2592–2602.

[8] Srebro, M.; Autschbach, J. Does a Molecule-Specific Density Functional Give an Accurate Electron Density? The Challenging Case of the CuCl Electric Field Gradient. *J. Phys. Chem. Lett.* **2012**, *3*, 576–581.

[9] Medvedev, M. G.; Bushmarinov, I. S.; Sun, J.; Perdew, J. P.; Lyssenko, K. A. Density functional theory is straying from the path toward the exact functional. *Science* **2017**, *355*, 49–52.

[10] Yu, X.; Sergentu, D.-C.; Feng, R.; Autschbach, J. Covalency of Trivalent Actinide Ions with Different Donor Ligands: Do Density Functional and Multireference Wavefunction Calculations Corroborate the Observed 'Breaks'?. *Inorg. Chem.* **2021**, *60*, 17744–17757.

[11] Szilagyi, R. K.; Metz, M.; Solomon, E. Spectroscopic Calibration of Modern Density Functional Methods Using [CuCl4]2-. *J. Phys. Chem.* **A 2002**, *106*, 2994–3007.

[12] Duignan, T. J.; Autschbach, J. Impact of the Kohn-Sham Delocalization Error on the 4f Shell Localization and Population in Lanthanide Complexes. *J. Chem. Theory Comput.* **2016**, *12*, 3109–3121.

[13] Frisch, M. J.; Trucks, G. W.; Schlegel, H. B.; Scuseria, G. E.; Robb, M. A.; Cheeseman, J. R.; Scalmani, G.; Barone, V.; Petersson, G. A.; Nakatsuji, H.; Li, X.; Caricato, M.; Marenich, A. V.; Bloino, J.; Janesko, B. G.; Gomperts, R.; Mennucci, B.; Hratchian, H. P.; Ortiz, J. V.; Izmaylov, A. F.; Sonnenberg, J. L.; Williams-Young, D.; Ding, F.; Lipparini, F.; Egidi, F.; Goings, J.; Peng, B.; Petrone, A.; Henderson, T.; Ranasinghe, D.; Zakrzewski, V. G.; Gao, J.; Rega, N.; Zheng, G.; Liang, W.; Hada, M.; Ehara, M.; Toyota, K.; Fukuda, R.; Hasegawa, J.; Ishida, M.; Nakajima, T.; Honda, Y.; Kitao, O.; Nakai, H.; Vreven, T.; Throssell, K.; Montgomery, J. A. Jr.; Peralta, J. E.; Ogliaro, F.; Bearpark, M. J.; Heyd, J. J.; Brothers, E. N.; Kudin, K. N.; Staroverov, V. N.; Keith, T. A.; Kobayashi, R.; Normand, J.; Raghavachari, K.; Rendell, A. P.; Burant, J. C.; Iyengar, S. S.; Tomasi, J.; Cossi, M.; Millam, J. M.; Klene, M.; Adamo, C.;

Cammi, R.; Ochterski, J. W.; Martin, R. L.; Morokuma, K.; Farkas, O.; Foresman, J. B.; Fox, D. J. "Gaussian 16 Revision C.01", Gaussian, Inc., Wallingford CT, 2016. URL: www.gaussian.com.

[14] Glendening, E. D.; Landis, C. R.; Weinhold, F. Natural bond orbital methods. *Wiley Interdiscip. Rev.: Comput. Mol. Sci.* **2012**, *2*, 1–42.

[15] Glendening, E. D.; Landis, C. R.; Weinhold, F. NBO 6.0: Natural bond orbital analysis program. *J. Comput. Chem.* **2013**, *34*, 1429–1437.

[16] Neese, F. Software update: The ORCA program system-Version 5.0. *Wiley Interdiscip. Rev.: Comput. Mol. Sci.* **2022**, *12*, e1606.

[17] Werner, H.-J.; Knowles, P. J.; Manby, F. R.; Black, J. A.; Doll, K.; Heßelmann, A.; Kats, D.; Köhn, A.; Korona, T.; Kreplin, D. A.; Ma, Q.; Miller, T. F.; Mitrushchenkov, A.; Peterson, K. A.; Polyak, I.; Rauhut, G.; Sibaev, M. The Molpro quantum chemistry package. *J. Chem. Phys.* **2020**, *152*,.

[18] Werner, H.-J.; Knowles, P. J.; Knizia, G.; Manby, F. R.; Schütz, M. Molpro: a general-purpose quantum chemistry program package. *WIREs Comput. Mol. Sci.* **2012**, *2*, 242–253.

[19] Werner, H. J.; Knowles, P. J.; Celani, P.; Györffy, W.; Hesselmann, A.; Kats, D.; Knizia, G.; Köhn, A.; Korona, T.; Kreplin, D.; Lindh, R.; Ma, Q.; Manby, F. R.; Mitrushenkov, A.; Rauhut, G.; Schütz, M.; Shamasundar, K. R.; Adler, T.; Amos, R. D.; Bennie, S. J.; Bernhardsson, A.; Berning, A.; Black, J. A.; Bygrave, P. J.; Cimiraglia, R.; Cooper, D. L.; Coughtrie, D.; Deegan, M. J. O.; Dobbyn, A. J.; Doll, K.; Dornbach, M.; Eckert, F.; Erfort, S.; Goll, E.; Hampel, C.; Hetzer, G.; Hill, J. G.; Hodges, M.; Hrenar, T.; Jansen, G.; Köppl, C.; Kollmar, C.; Lee, S. J. R.; Liu, Y.; Lloyd, A. W.; Mata, R. A.; May, A. J.; Mussard, B.; McNicholas, S. J.; Meyer, W.; Miller III, T. F.; Mura, M. E.; Nicklass, A.; O'Neill, D. P.; Palmieri, P.; Peng, D.; Peterson, K. A.; Pflüger, K.; Pitzer, R.; Polyak, I.; Reiher, M.; Richardson, J. O.; Robinson, J. B.; Schröder, B.; Schwilk, M.; Shiozaki, T.; Sibaev, M.; Stoll, H.; Stone, A. J.; Tarroni, R.; Thorsteinsson, T.; Toulouse, J.; Wang, M.; Welborn, M.; Ziegler, B. "MOLPRO, version, a package of ab initio programs", .

[20] Becke, A. D. Density–functional thermochemistry. III. The role of exact exchange. *J. Chem. Phys.* **1993**, *98*, 5648–5652.

[21] Schäfer, A.; Horn, H.; Ahlrichs, R. Fully Optimized Contracted Gaussian Basis Sets for Atoms Li to Kr.. *J. Chem. Phys.* **1992**, *97*, 2571–2577.

[22] Schäfer, A.; Huber, C.; Ahlrichs, R. Fully Optimized Contracted Gaussian Basis Sets of Triple Zeta Valence Quality for Atoms Li to Kr. *J. Chem. Phys.* **1994**, *100*, 5829–5835.

[23] Weigend, F.; Ahlrichs, R. Balanced basis sets of split valence, triple zeta valence and quadruple zeta valence quality for H to Rn: Design and assessment of accuracy. *Phys. Chem. Chem. Phys.* **2005**, *7*, 3295–3305.

[24] Grimme, S.; Antony, J.; Ehrlich, S.; Krieg, H. A consistent and accurate ab initio parametrization of density functional dispersion correction (DFT-D) for the 94 elements H-Pu. *J. Chem. Phys.* **2010**, *132*, 154104.

[25] Grimme, S.; Ehrlich, S.; Goerigk, L. Effect of the damping function in dispersion corrected density functional theory. *J. Comput. Chem.* **2011**, *32*, 1456–1465.

[26] Peverati, R.; Truhlar, D. G. Quest for a Universal Density Functional: The Accuracy of Density Functionals across a Broad Spectrum of Databases in Chemistry and Physics. *Phil. Trans. R. Soc. A* **2014**, *372*, 20120476.

[27] Witte, J.; Goldey, M.; Neaton, J. B.; Head-Gordon, M. Beyond Energies: Geometries of Nonbonded Molecular Complexes as Metrics for Assessing Electronic Structure Approaches. *J. Chem. Theory Comput.* **2015**, *11*, 1481–1492.

[28] Sirianni, D. A.; Alenaizan, A.; Cheney, D. L.; Sherrill, C. D. Assessment of Density Functional Methods for Geometry Optimization of Bimolecular van Der Waals Complexes. *J. Chem. Theory Comput.* **2018**, *14*, 3004–3013.

[29] Morgante, P.; Peverati, R. Statistically Representative Databases for Density Functional Theory Via Data Science. *Phys. Chem. Chem. Phys.* **2019**, *21*, 19092–19103.

[30] Kesharwani, M. K.; Brauer, B.; Martin, J. M. L. Frequency and Zero-Point Vibrational Energy Scale Factors for Double-Hybrid Density Functionals (and Other Selected Methods): Can Anharmonic Force Fields Be Avoided?. *J. Phys. Chem. A* **2015**, *119*, 1701–1714.

[31] Hellweg, A.; Hättig, C.; Höfener, S.; Klopper, W. Optimized accurate auxiliary basis sets for RI-MP2 and RI-CC2 calculations for the atoms Rb to Rn. *Theor. Chem. Acc.* **2007**, *117*, 587–597.

[32] Eichkorn, K.; Treutler, O.; Öhm, H.; Häser, M.; Ahlrichs, R. Auxiliary Basis Sets to Approximate Coulomb Potentials. *Chem. Phys. Lett.* **1995**, *242*, 652–660.

[33] Eichkorn, K.; Weigend, F.; Treutler, O.; Ahlrichs, R. Auxiliary basis sets for main row atoms and transition metals and their use to approximate Coulomb potentials. *Theor. Chem. Acc.* **1997**, *97*, 119–124.

[34] Eichkorn, K.; Treutler, O.; Öhm, H.; Häser, M.; Ahlrichs, R. Auxiliary basis sets to approximate Coulomb potentials (Erratum: *ibid.* **242** (1995) 652). *Chem. Phys. Lett.* **1995**, *240*, 283–290.

[35] Weigend, F. Accurate Coulomb-fitting basis sets for H to Rn. *Phys. Chem. Chem. Phys.* **2006**, *8*, 1057–1065.

[36] Lee, C.; Yang, W.; Parr, R. G. Development of the Colle-Salvetti correlation-energy formula into a functional of the electron density. *Phys. Rev. B* **1988**, *37*, 785–789.

[37] Becke, A. D. Density-functional exchange-energy approximation with correct asymptotic behavior. *Phys. Rev. A* **1988**, *38*, 3098–3100.

[38] Adamo, C.; Barone, V. Toward reliable density functional methods without adjustable parameters: The PBE0 model. *J. Chem. Phys.* **1999**, *110*, 6158–6170.

[39] Yanai, T.; Tew, D. P.; Handy, N. C. A new hybrid exchange–correlation functional using the Coulomb-attenuating method (CAM-B3LYP). *Chem. Phys. Lett.* **2004**, *393*, 51–57.

[40] Takano, Y.; Houk, K. N. Benchmarking the Conductor-like Polarizable Continuum Model (CPCM) for Aqueous Solvation Free Energies of Neutral and Ionic Organic Molecules. *J. Chem. Theory Comput.* **2005**, *1*, 70–77.

[41] Mennucci, B. Polarizable continuum model. *WIREs Comput. Mol. Sci.* **2012**, *2*, 386–404.

[42] Cybulski, S. M.; Bishop, D. M. Theory of relaxed density matrices: Application to second-order response properties. *Int. J. Quantum Chem.* **1994**, *49*, 371–381.

[43] Bousquet, D.; Brémond, E.; Sancho-García, J. C.; Ciofini, I.; Adamo, C. Is There Still Room for Parameter Free Double Hybrids? Performances of PBE0-DH and B2PLYP over Extended Benchmark Sets. *J. Chem. Theory Comput.* **2013**, *9*, 3444–3452.

[44] Møller, C.; Plesset, M. S. Note on an approximation treatment for many-electron systems. *Phys. Rev.* **1934**, *46*, 618–622.

[45] Piris, M. Dynamic electron-correlation energy in the natural-orbital-functional second-order-Møller-Plesset method from the orbital-invariant perturbation theory. *Phys. Rev. A* **2018**, *98*,.

[46] Azhary, A. E.; Rauhut, G.; Pulay, P.; Werner, H. Analytical energy gradients for local second-order Møller-Plesset perturbation theory. *J. Chem. Phys.* **1998**, *108*, 5185.

[47] Riplinger, C.; Neese, F. An efficient and near linear scaling pair natural orbital based local coupled cluster method. *J. Chem. Phys.* **2013**, *138*,.

[48] Mizukami, W.; Mitarai, K.; Nakagawa, Y. O.; Yamamoto, T.; Yan, T.; Ohnishi, Y.-y. Orbital optimized unitary coupled cluster theory for quantum computer. *Phys. Rev. Res.* **2020**, *2*,.

[49] Bartlett, R. J.; Musiał, M. Coupled-cluster theory in quantum chemistry. *Rev. Mod. Phys.* **2007**, *79*, 291–352.

[50] Raghavachari, K.; Trucks, G. W.; Pople, J. A.; Head-Gordon, M. A fifth-order perturbation comparison of electron correlation theories. *Chem. Phys. Lett.* **1989**, *157*, 479–483.

[51] Jiang, W.; DeYonker, N. J.; Wilson, A. K. Multireference character for 3D transition-metal-containing molecules. *J. Chem. Theory Comput.* **2012**, *8*, 460–468.

[52] Wang, J.; Manivasagam, S.; Wilson, A. K. Multireference character for 4D transition metal-containing molecules. *Journal of Chemical Theory and Computation* **2015**, *11*, 5865–5872.

[53] Stephens, P. J.; Devlin, F. J.; Chabalowski, C. F.; Frisch, M. J. Ab initio calculation of vibrational absorption and circular dichroism spectra using density functional force fields. *J. Phys. Chem. A* **1994**, *98*, 11623–11627.

[54] Perdew, J. P.; Burke, K.; Ernzerhof, M. Generalized Gradient Approximation Made Simple. *Phys. Rev. Lett.* **1996**, *77*, 3865–3868.

[55] Perdew, J. P.; Burke, K.; Ernzerhof, M. Generalized Gradient Approximation Made Simple (Erratum). *Phys. Rev. Lett.* **1997**, *78*, 1396.

[56] Becke, A. D. A new mixing of Hartree-Fock and local density-functional theories. *J. Chem. Phys.* **1993**, *98*, 1372–1377.

[57] Grimme, S. Semiempirical hybrid density functional with perturbative second-order correlation. *J. Chem. Phys.* **2006**, *124*, 034108 (16 pages).

[58] Beattie, J. K.; Moore, C. J. Crystal and molecular structures of rinneite, sodium tripotassium hexachloroferrate(II), and hexaamminecobalt(III) hexachloroferrate(III). Comparison of iron-chloride distances in hexachloroferrate(II) and hexachloroferrate(III). *Inorg. Chem.* **1982**, *21*, 1292–1295.

[59] Lee, T. J.; Taylor, P. R. A diagnostic for determining the quality of single-reference electron correlation methods. *Int. J. Quantum Chem.* **1989**, *36*, 199–207.

[60] Meister, J.; Schwarz, W. H. E. Principal components of ionicity. *J. Phys. Chem.* **1994**, *98*, 8245–8252.

[61] Cho, M.; Sylvetsky, N.; Eshafi, S.; Santra, G.; Efremenko, I.; Martin, J. M. L. The Atomic Partial Charges Arboretum: Trying to See the Forest for the Trees. *ChemPhysChem* **2020**, *21*, 688–696.

[62] Debefve, L. M.; Pollock, C. J. Systematic assessment of DFT methods for geometry optimization of mononuclear platinum-containing complexes. *Phys. Chem. Chem. Phys.* **2021**, *23*, 24780–24788.

[63] Adamo, C.; Barone, V. Toward chemical accuracy in the computation of NMR shieldings: the PBE0 model. *Chem. Phys. Lett.* **1998**, *298*, 113–119.

[64] Holmes, S. T.; Schönzart, J.; Philips, A. B.; Kimball, J. J.; Termos, S.; Altenhof, A. R.; Xu, Y.; O'Keefe, C. A.; Autschbach, J.; Schurko, R. W. Structure and Bonding in Rhodium Coordination Compounds: A ^{103}Rh Solid-State NMR and Relativistic DFT Study. *Chem. Sci.* **2024**, *15*, 2181–2196.

[65] Carter-Fenk, K.; Lao, K. U.; Liu, K.-Y.; Herbert, J. M. Accurate and Efficient ab Initio Calculations for Supramolecular Complexes: Symmetry-Adapted Perturbation Theory with Many-Body Dispersion. *J. Phys. Chem. Lett.* **2019**, *10*, 2706–2714.

[66] Prasad, V. K.; Pei, Z.; Edelmann, S.; Otero-de-la Roza, A.; DiLabio, G. A. BH9, a New Comprehensive Benchmark Data Set for Barrier Heights and Reaction Energies: Assessment of Density Functional Approximations and Basis Set Incompleteness Potentials. *J. Chem. Theory Comput.* **2021**, *18*, 151–166.

[67] Sandler, I.; Chen, J.; Taylor, M.; Sharma, S.; Ho, J. Accuracy of DLPNO-CCSD(T): Effect of Basis Set and System Size. *J. Phys. Chem. A* **2021**, *125*, 1553–1563.

[68] Taube, A. G.; Bartlett, R. J. Rethinking linearized coupled-cluster theory. *J. Chem. Phys.* **2009**, *130*,.

[69] Hrobarik, P.; Hrobarikova, V.; Greif, A. H.; Kaupp, M. Giant Spin-Orbit Effects on NMR Shifts in Diamagnetic Actinide Complexes: Guiding the Search of Uranium(VI) Hydride Complexes in the Correct Spectral Range. *Angew. Chem. Int. Ed.* **2012**, *51*, 10884–10888.

[70] Panetti, G. B.; Sergentu, D.-C.; Gau, M. R.; Carroll, P. J.; Autschbach, J.; Walsh, P. J.; Schelter, E. J. Isolation and Characterization of a Covalent Ce(IV)-Aryl Complex with an Anomalous 13C Chemical Shift. *Nat. Commun.* **2021**, *12*, 1713 (7 pages).

[71] Greif, A.; Hrobarik, P.; Autschbach, J.; Kaupp, M. Giant Spin-Orbit Effects on 1H and 13C NMR Shifts for Uranium(VI) Complexes Revisited: Role of the Exchange-Correlation Response Kernel, Bonding Analyses, and New Predictions. *Phys. Chem. Chem. Phys.* **2016**, *18*, 30462–30474.

[72] Prokopiou, G.; Autschbach, J.; Kronik, L. Assessment of the performance of optimally-tuned range-separated hybrid functionals for nuclear magnetic shielding calculations. *Adv. Theory Simul.* **2020**, *3*, 2000083 (8 pages).

[73] Sai, N.; Barbara, P. F.; Leung, K. Hole Localization in Molecular Crystals from Hybrid Density Functional Theory. *Phys. Rev. Lett.* **2011**, *106*, 226403–4.

[74] Baer, R.; Livshits, E.; Salzner, U. Tuned Range-Separated Hybrids in Density Functional Theory. *Ann. Rev. Phys. Chem.* **2010**, *61*, 85–109.

[75] Perdew, J. P.; Ruzsinszky, A.; Constantin, L. A.; Sun, J.; Csonka, G. I. Some Fundamental Issues in Ground-State Density Functional Theory: A Guide for the Perplexed. *J. Chem. Theory Comput.* **2009**, *5*, 902–908.

[76] Jaramillo, J.; Scuseria, G. E.; Ernzerhof, M. Local hybrid functionals. *J. Chem. Phys.* **2003**, *118*, 1068–1073.

[77] Schattenberg, C. J.; Lehmann, M.; Bühl, M.; Kaupp, M. Systematic Evaluation of Modern Density Functional Methods for the Computation of NMR Shifts of 3d Transition-Metal Nuclei. *J. Chem. Theory Comput.* **2022**, *18*, 273–292.

[78] Center for Computational Research, University at Buffalo. URL `http://hdl.handle.net/10477/79221`. Accessed 2024/02.

TOC Synopsis and TOC Graphics

The ‘dative’ covalent interactions between metals and ligands in coordination compounds, i.e., donation and back-donation, are manifestations of electron delocalization and subject to errors in approximate calculations. This work addresses the extent of donation/back-donation in a series of closed-shell complexes. A number of Kohn-Sham density functionals and post-Hartree-Fock methods are assessed in comparison to relaxed CCSD(T) densities.

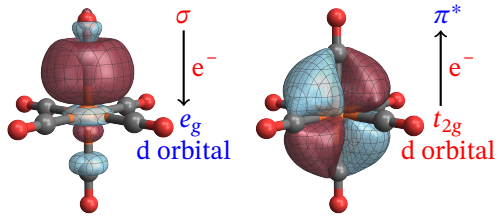

L → M σ-Donation M → L π-Back-Donation

How much electron density is donated?